NeuroImage 83 (2013) 581–592

Contents lists available at ScienceDirect

NeuroImage

journal homepage: www.elsevier.com/locate/ynimg

Multiphasic modification of intrinsic functional connectivity of the rat brain during increasing levels of propofol

Xiping Liu [a], Siveshigan Pillay [b], Rupeng Li [b], Jeannette A. Vizuete [a,c], Kimberly R. Pechman [d], Kathleen M. Schmainda [b,e], Anthony G. Hudetz [a,b,*]

[a] Department of Anesthesiology, Medical College of Wisconsin, USA
[b] Department of Biophysics, Medical College of Wisconsin, USA
[c] Department of Biomedical Engineering, Marquette University, USA
[d] Department of Neurosurgery, Medical College of Wisconsin, USA
[e] Department of Radiology, Medical College of Wisconsin, USA

ARTICLE INFO

Article history:
Accepted 1 July 2013
Available online 10 July 2013

Keywords:
Propofol anesthesia
Functional connectivity
Resting state
Simultaneous fMRI and EEG
Consciousness

ABSTRACT

The dose-dependent effects of anesthetics on brain functional connectivity are incompletely understood. Resting-state functional magnetic resonance imaging (rsfMRI) is widely used to assess the functional connectivity in humans and animals. Propofol is an anesthetic agent with desirable characteristics for functional neuroimaging in animals but its dose-dependent effects on rsfMRI functional connectivity have not been determined. Here we tested the hypothesis that brain functional connectivity undergoes specific changes in distinct neural networks at anesthetic depths associated with loss of consciousness. We acquired spontaneous blood oxygen level-dependent (BOLD) signals simultaneously with electroencephalographic (EEG) signals from rats under steady-state, intravenously administered propofol at increasing doses from light sedation to deep anesthesia (20, 40, 60, 80, and 100 mg/kg/h IV). Power spectra and burst suppression ratio were calculated from the EEG to verify anesthetic depth. Functional connectivity was determined from the whole brain correlation of BOLD data in regions of interest followed by a segmentation of the correlation maps into anatomically defined regional connectivity. We found that propofol produced multiphasic, dose dependent changes in functional connectivity of various cortical and subcortical networks. Cluster analysis predicted segregation of connectivity into two cortical and two subcortical clusters. In one cortical cluster (somatosensory and parietal), the early reduction in connectivity was followed by transient reversal; in the other cluster (sensory, motor and cingulate/retrosplenial), this rebound was absent. The connectivity of the subcortical cluster (brainstem, hippocampal and caudate) was strongly reduced, whereas that of another (hypothalamus, medial thalamus and n. basalis) did not. Subcortical connectivity increased again in deep anesthesia associated with EEG burst suppression. Regional correlation analysis confirmed the breakdown of connectivity within and between specific cortical and subcortical networks with deepening propofol anesthesia. Cortical connectivity was suppressed before subcortical connectivity at a critical propofol dose associated with loss of consciousness.

Introduction

Since the discovery by Biswal (Biswal et al., 1995), "resting state" functional magnetic resonance imaging (fMRI) during a stimulus- or task-free condition has become a popular method for assessing functional connectivity patterns of the brain. As it has been demonstrated, the spatial correlation of low-frequency (<1 Hz) spontaneous fluctuations in blood oxygen level-dependent BOLD signals delineates large-scale networks of the brain that can be identified by various sensory, motor, and cognitive functions (Gusnard and Raichle, 2001; Power et al., 2011; Raichle et al., 2001). Because resting-state fMRI (rsfMRI) can be performed without subject response or participation, it has been applied to assess brain function in non-communicating patients in conditions such as sleep, anesthesia, vegetative state, and coma (Boly et al., 2012a; Duyn, 2011; Heine et al., 2012; Hudetz, 2012). Most of these studies aimed to determine if there were specific patterns of BOLD functional connectivity associated with the change in state of consciousness, but the results obtained so far have been controversial.

Resting state fMRI has been also performed in animals; mostly under general anesthesia (Hutchison et al., 2010; Liu et al., 2011; Lu et al., 2007; Pawela et al., 2008, 2009; Tu et al., 2011; Williams et al., 2010; Zhao et al., 2008), and in a few cases, in wakefulness (Liang et al., 2011; Zhang et al., 2010). As in humans, various intrinsic networks have been identified in both primates (Dawson et al., 2012; Mantini et al., 2011) and rodents (Keilholz et al., 2012; Lu et al., 2012; Pawela et al., 2008). Some studies in rodents found that in deep surgical

* Corresponding author at: Department of Anesthesiology, Medical College of Wisconsin, 8701 Watertown Plank Road, Milwaukee, WI 53226, USA. Fax: +1 414 456 6507.
E-mail address: ahudetz@mcw.edu (A.G. Hudetz).

1053-8119/$ – see front matter © 2013 Elsevier Inc. All rights reserved.
http://dx.doi.org/10.1016/j.neuroimage.2013.07.003

anesthesia functional connectivity was largely diminished (Lu et al., 2007; Wang et al., 2011; Williams et al., 2010). Because most animal studies were performed at a single anesthetic dose (Kalthoff et al., 2011; Zhou et al., 2008) or at relatively deep anesthesia (Liu et al., 2012b), the potentially more subtle, dose-dependent modulation of functional connectivity at graded levels of anesthesia relevant to a change in state of consciousness remains unclear.

To fill this gap in knowledge, we investigated the dose-dependent effect of the intravenous anesthetic propofol (2,6-diisopropylphenol) on rsfMRI functional connectivity in the rat. We chose propofol because it is a common, clinically used anesthetic, it has been used in several recent neuroimaging studies in humans (Boveroux et al., 2010; Liu et al., 2012a; Schrouff et al., 2011), and it is a potentially useful anesthetic for animal imaging studies as well. Neuroimaging data under propofol anesthesia in animals are scarce. An investigation with resting-state imaging (Tu et al., 2011) in the rat found a suppression of thalamocortical functional connectivity at a high propofol dose corresponding to deep surgical anesthesia. Functional connectivity in rodents at moderate doses of propofol most relevant to anesthetic state modulations has not been investigated. We hypothesized that the observed changes in brain functional connectivity may depend on the anesthetic depth and that these changes may be different in various intrinsic networks. In fact, as we will show, the dose-dependent effect of propofol on functional connectivity is not gradual, but characterized by complex, multiphasic changes as a function of increasing propofol dose in the rat brain.

Methods

Animals

All experimental procedures and protocols were approved by the Institutional Animal Care and Use Committee of the Medical College of Wisconsin (Milwaukee, Wisconsin). All procedures conformed to the Guiding Principles in the Care and Use of Animals of the American Physiologic Society and were in accordance with the Guide for the Care and Use of Laboratory Animals.

Experiments were performed on 7, naïve, adult (280–350 g), male, Sprague–Dawley rats (Harlan Laboratories). All animals were housed in a reverse light–dark cycle room for at least 10 days prior to experiment. Food and water access was ad libitum.

Surgical preparation

The surgical protocol was performed on the day of each experiment. Animals were initially anesthetized, in an induction box, with 5% isoflurane; the hair on the surgical sites (right inner thigh and head) was shaved. They were then transferred to a stereotaxic frame, where isoflurane (1.9 ± 0.2%), distributed via a gas anesthesia mask (Model 929-B Rat Gas Anesthesia Head Holder, David Kopf Instruments, Tujunga, CA), vaporized into a mixture of 30% O_2, 70% N_2 and delivered at a flow rate of 5 L/min was continued for maintenance during surgery. Core body temperature was rectally monitored (model 73A, YSI Yellow Springs, OH) and maintained at 37 ± 0.5 °C with a thermostat-controlled, electric (TC-1000, CWE Inc., Ardmore, PA) heating pad.

For electrode implantation, sterile, 0.5% bupivacaine was administered subcutaneously for local anesthesia, and the cranium revealed by laterally reflecting skin and connective tissue. To maintain adequate MR-image quality hydrogen peroxide and/or a cautery were used to minimize bleeding. To verify the depth of anesthesia, commercially available MR-compatible Teflon-coated, bipolar platinum–iridium electrodes (Plastics One Inc., Roanoke, VA), whose tips (~1 mm) were stripped of any Teflon insulation and bent at a 45° to protect the integrity of the dura, were implanted through burr holes, created using an electric drill, in the cranium. All electrodes were manually inserted over the left frontal cortex (AP = +4.0 and 6.1, L = −2.34) such that the structural integrity of the right hemisphere was not disturbed. To secure the wires in place, commercially available cyanoacrylate adhesive (Krazy Glue, Columbus, OH), used due to preliminary experiments that indicated minimal adhesive-induced artifact, was applied around the electrode and burr hole.

The animal was then transferred to a heated surgical table. The right femoral vein and femoral artery were cannulated with PE-50 polyethylene tubing (Becton-Dickinson, Sparks, MD), flushed previously with heparinized saline for intravenous propofol delivery and arterial blood pressure monitoring, respectively. Finally, a tracheostomy was performed for mechanical ventilation.

MRI hardware preparation and physiological monitoring

All fMRI data were acquired on a Bruker 9.4 T (AVANCE; Bruker, Billerica, MA, USA) scanner using a Bruker linear transmit coil (T10325) and rodent surface-receiving coil (T9208). The animal was transferred to a custom-built G-10 fiberglass MR imaging cradle. Rats continued to receive isoflurane in a 70/30 N_2/O_2 gas mixture, through an intra-tracheal Y-shaped Teflon tube at 50–60 pushes per minute and 3.5–4.5 ml tidal volume, using a volume-cycled MR-compatible rodent ventilator (CWE, Ardmore, PA). The isoflurane gas mixture (assessed by monitoring the inspired and end-tidal O_2, CO_2 and isoflurane) and the ventilator parameters were adjusted according to the physiology of each animal. As isoflurane was gradually discontinued, intravenous (*IV*) delivery of a mixture of 20 mg/ml propofol and 1 mg/ml pancuronium bromide (in 2:1 volume ratio) commenced.

The rats' core temperature was monitored, with a rectal thermometer, and maintained at 37 ± 0.5 °C by a water-pump driven temperature regulator (Medi-therm III, Gaymar Industries, Orchard Park, NY). A small animal monitoring system (Model 1025, SA Instruments, Stony Brook, NY) was used to monitor arterial blood pressure, core temperature, and respiratory rate. Pulse oximetry (8600 V, Nonin Medical, Plymouth, MN), inspired/expired O_2 and CO_2 (POET IQ2, Criticare Systems, Waukesha, WI), and heart rate were also acquired. All physiological variables were kept close to normative levels throughout the duration of the experiment protocol, and acquired using WINDAQ software (DATAQ Instruments, Akron, OH).

fMRI protocol

All animals received a continuous infusion of propofol (administered sequentially: 20, 40, 60, 80, and 100 mg/kg/h IV). The propofol dose was adjusted by changing the infusion rate on a MR-compatible syringe pump (Harvard Apparatus, Holliston, MA). To eliminate spontaneous respirations and minimize motion artifacts, the muscle relaxant, pancuronium bromide was added to the propofol infusion. Rats were weaned off the isoflurane mixture as soon as their physiological parameters were stable enough to introduce the propofol and pancuronium bromide mixture. Isoflurane was discontinued for 40 min prior to the onset of functional data acquisition. Fig. 1A summarizes the timeline of the fMRI study.

Image acquisition began once the rat reached steady state (as confirmed with the EEG signal) at the lightest dose (20 mg/kg/h). After a localization scan with the fast low angle shot (FLASH) sequence, a relaxation enhancement rapid acquisitions (RARE) pulse sequence was applied to acquire the high-resolution anatomical scan as 9 contiguous sagittal slices (center of the 5th slice in alignment with animal midline) with the following acquisition parameters: repetition time (TR) of 5000 ms, echo time (TE) of 11.3 ms, number of averages = 2, RARE factor of 8, field of view (FOV) of 35 × 35 mm^2, matrix size of 256 × 256, and slice thickness of 1 mm. After the high-resolution anatomical scan, a series of functional scans were taken with a single-shot echo-planar imaging (EPI) sequence. Using the same geometry as that of the anatomy, the scan parameters of each functional resting session were as follows: TR of 2000 ms, TE of 19.5 ms, single average, 110 repetitions and matrix size of 96 × 96. There were 5 resting scans

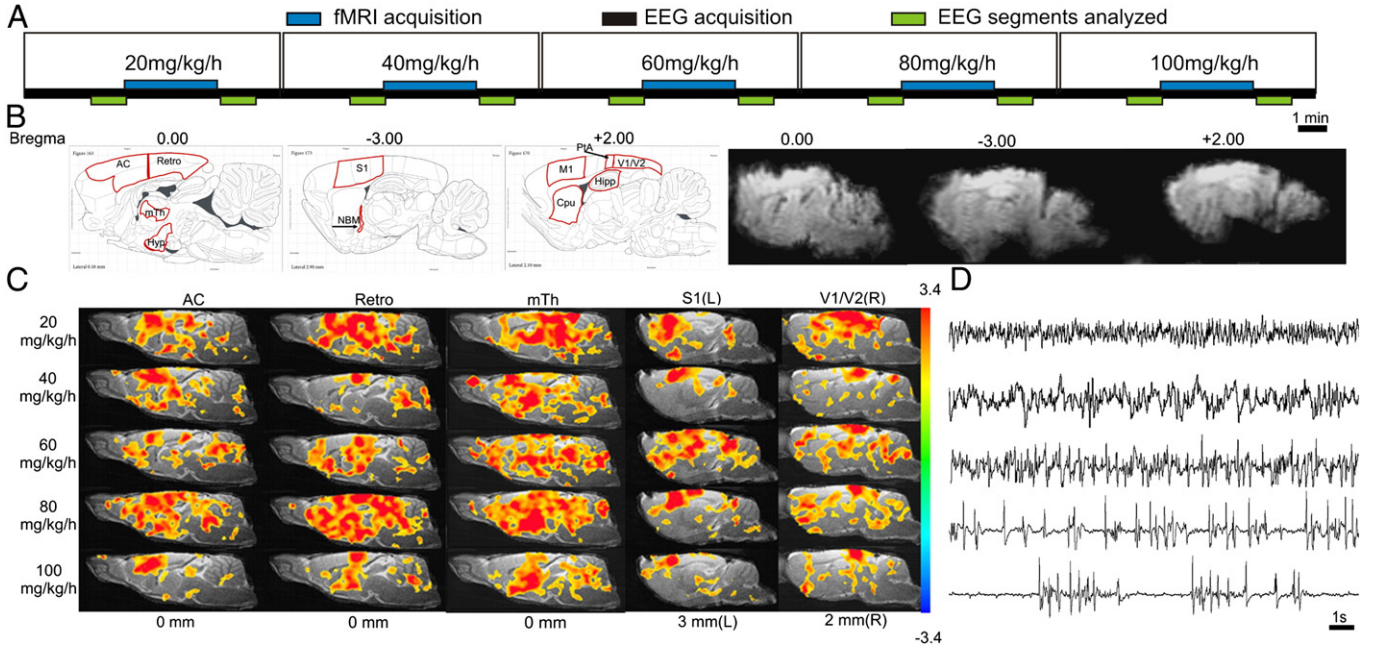

Fig. 1. Resting state network (RSN) analysis using select seed regions of interest (ROI). A. Time line of the fMRI experiment. The electroencephalogram was continuously recorded throughout the experiment; the EEG segments used for the analyses are indicated by the green solid bars. Each animal received five doses of propofol that increased incrementally from 20 to 100 mg/kg/h. Steady state, as determined by the EEG, occurred within 10 min of a change in propofol dose. Resting functional scans were acquired after steady state was achieved at each propofol dose. The total duration of each experiment was approximately 75 min. B. Left: Schematic of seed ROI selection overlaid on a stereotaxic drawing from the Paxinos rat brain atlas. Right: Corresponding EPI images for image quality demonstration. C. RSN maps at five propofol doses (shown on the left) for the selected seed ROIs (shown on the top), each from the same slice location (shown at the bottom with reference to midline), superimposed on the anatomic template images, and scaled according to the color bar (on the right). Seed ROIs: anterior cingulate (AC), retrosplenium (Retro), medial thalamus (mTh), left primary somatosensory cortex (S1), and right visual cortex (V1/V2). For each seed, only one of the 9 image slices is shown. Results represent an average from 7 animals. D. Raw EEG traces from a representative rat at each propofol dose. Desynchronized, low-amplitude high-frequency activity at 20 mg/kg/h (conscious sedation), low-frequency activity at 40–60 mg/kg/h (LOC), and deep anesthesia with burst suppression at 80–100 mg/kg/h.

total (1 at each propofol dose). At the end of each resting scan, the propofol dose was increased incrementally. Animals were allowed 10 min to equilibrate at each new propofol dose prior to the onset of subsequent resting scans.

Restraint and gradient induced stress

The effects of potential stress from mechanical head restraint and scanner gradient noise were examined in a separate group of 4 rats (non-paralyzed, and outside the scanner) at the two lowest propofol doses. The animals were equipped with frontal EEG leads the same way as in the FMRI experiments. Gradient noise was digitally recorded using an omnidirectional condenser microphone (MT830R, Audio-Technica, Stow, OH) and digital portastudio (TASCAM DP-01FC, TEAC America Inc, Montebello, CA) played back at equal sound level during the bench experiments. Head restraint was applied in a similar manner to that in the scanner environment. The animals' level of arousal was assessed using a behavioral response battery developed previously (Jugovac et al., 2006). Specifically, responses to vibrissal, olfactory, corneal, and tail stimulation were scored on a scale from 2 (completely preserved response) to 0 (completely abolished response). The testing procedure was repeated three times at each propofol dose in three conditions in this order: (1) unrestrained, (2) exposed to gradient noise, and (3) exposed to gradient noise and head-restraint (the response to head restraint alone was not tested in order to limit the duration of anesthetic exposure).

EEG acquisition

The MR-compatible two-channel connector cable was threaded over the electrode pedestal and fed into a standard stimulate/record switching unit (SRS unit, Grass Technologies, West Warwick, RI). The male output cable from this unit terminated, via another shielded input cable (CAB-21572, Grass Technologies), on a Grass QP511 Quad AC Amplifier (Grass Technologies). The signal was amplified at 20,000 times, analog band-pass filtered at 1–300 Hz, analog notch filtered at 60 Hz, and digitally sampled at 500 Hz using WINDAQ. EEG signal was acquired continuously throughout the experiment and served as a guide when determining whether steady state propofol was achieved at each dose prior to functional image acquisition.

Data analysis and statistics: EEG

EEG analyses were only carried out on segments of data immediately before and after image acquisition to ensure that these segments were free from gradient induced artifact. The EEG data were chosen at a consistent time-point across all animals; they were obtained during steady state at each respective dose of propofol for every animal. Preliminary exploration of the data revealed that the power spectra from segments before and after each resting scan were similar. Individual band powers were normalized for each rat at every propofol dose by dividing each band power by total power and multiplying by the total power from all animals. A grand average of the normalized individual band power at each propofol dose was then used for the ensuing analyses. All electroencephalographic data were analyzed using custom scripts in MATLAB version 7.3.0 (MathWorks Inc., Natick, MA).

Power spectra were calculated from segments of EEG data using Welch's spectral estimation method with a 250-point window and 90% overlap. To reduce the impact of spectral leakage, a Hanning window was used. Band powers (δ = 1–4 Hz, θ = 5–7 Hz, α = 8–12 Hz, β = 13–30 Hz, low-gamma L-γ = 30–50 Hz, and high-gamma H-γ = 70–140 Hz) were obtained from the spectra by averaging signal power in the respective frequency ranges.

As the deeper levels of anesthesia were reached, the EEG was characterized by high amplitude (burst) activity interrupted by low

amplitude (suppression) activity; this pattern alternated. The burst suppression ratio (BSR) was defined as the ratio between the summation of the suppressed period and the entire epoch length (Eq. (1)):

$$BSR = \frac{\text{Total time spent in suppression}}{\text{Epoch length}}. \quad (1)$$

The start of a suppression period was determined by examining when the EEG amplitude remained below a threshold value for a minimum of 0.6 s; the suppression period was defined as long as the amplitude remained below the threshold value. The start of a burst was defined when the amplitude rose above the threshold for the first time. Threshold values were unique to each rat in that they were defined as the rectified mean multiplied by the standard deviation of the EEG signal for each rat at each propofol dose. BSR data were normalized using the same method as that used for band power normalization.

All 7 rats were included in the data analyses. The effect of propofol dose on EEG band powers and BSR was tested with repeated measures Multivariate analysis of variance (MANOVA), with the dose as the independent variable, rat as the subject (random) variable, and band power and BSR as dependent variables. The omnibus test was followed by a Tukey–Kramer multiple-comparison post-hoc test on factors that showed a significant difference.

Statistical analyses were performed using NCSS 2007 (NCSS, Kaysville UT). All data are presented as ± standard deviation from the mean.

Data analysis and statistics: fMRI

The Analysis of Functional NeuroImages (AFNI) software package (NIH, Baltimore, MD) was used for data analyses. The anatomical image set of one rat was chosen as a reference template (matrix size 256 × 256 × 9). After slice-timing correction and motion correction, the registration tool, FLIRT, within the FSL software package was used to register all rats' fMRI images onto the reference template with higher spatial resolution.

Seed-based analyses were implemented to investigate the resting-state functional connectivity (FC) changes at each propofol dose. Twelve regions of interest (ROI), based on a priori information, were manually delineated as per the Paxinos rat brain atlas and chosen such that a range of neural functioning, shown to be altered by the presence of anesthesia, received adequate representation: the oral part of the pontine reticular nucleus (PnO), hypothalamus (Hypo), nucleus basalis of Meynert (NBM), and the medial thalamus (mTh), all critical components of the ascending arousal system, modulate cortical arousal and conscious state regulation (Alkire et al., 2008; Jones, 2003; Laureys, 2005); anterior cingulate (AC), parietal association cortex (PtA), retrosplenium (Retro), hippocampus (Hipp), and caudate putamen (CPu) are all implicated in information maintenance and integration, learning and memory, and self-referential processing (Ma et al., 2002; Raichle et al., 2001; Vincent et al., 2008); the motor cortex (M1), primary sensory cortex (S1), and visual cortices (V1/V2) encode and process sensory information (Alkire et al., 2008; Dean, 1990; Erchova et al., 2002). Only the AC, Retro, mTh, and Hypo were chosen along the midline, whereas the remaining ROIs were chosen separately in each hemisphere. Considering the size of each ROI, the effect of resampling the fMRI data to higher resolution on functional connectivity calculation should be negligible.

All resting-state fMRI data were motion-corrected, detrended, and frequency filtered (with low-pass filter of 0.08 Hz) before the FC computation. The power spectra were examined for all animals with cortical and subcortical ROIs to verify that the major contribution to power was below 0.08 Hz (Supplementary Fig. 1). Cross correlation, specifically Pearson correlation (r) was the primary statistical approach used to assess FC.

For each seed ROI, the averaged preprocessed time course from each seed region was used as reference, and then cross-correlated with each voxel preprocessed time course in the whole brain to form the FC (r values) maps for individual animals. All r values in the individual subject map were then transformed to Fisher's Z scores for normalization by using the relationship between Z score and r value:

$$Z = \frac{1}{2} * \ln \frac{1+r}{1-r}, \quad (2)$$

which yields variable Z that is approximately normally distributed. Finally all z maps were clustered with minimum cluster size of 42 voxels (clusterwise $P < 0.05$, simulated result with AlphaSim command in AFNI to allow the maximum cluster size that has clusterwise type one error $\alpha < 0.05$).

To analyze the similarity in ROI response patterns, K-means clustering (a method of cluster analysis which aims to partition n observations into k clusters in which each observation belongs to the cluster with the nearest mean) was used. Significant FC maps of each seed ROI were generated with threshold of fisher Z >= 0.5. The whole brain significantly (Z >= 0.5) connected voxel count (SCVC) was then acquired for each significant ROI FC map. As most animals started to show burst suppression on EEG at propofol levels of 80 and 100 mg/kg/h, which may imply a drastically different mechanism of brain network interaction compared to that at the lower propofol levels (20, 40, 60 mg/kg/h), we only applied the clustering to those three lower dose levels, when consciousness was of more relevance. The whole brain VC changes (difference between 40 and 20 vs. difference between 60 and 40 mg/kg/h) of each seed ROI (left and right combined) were clustered to identify groups of ROIs that have distinct dynamic FC change patterns with anesthetic dose (Fig. 4).

To further investigate the region-to-region connectivity change, individual significant whole brain FC maps of each seed ROI was segmented again into the 12, abovementioned, target regions to get regional SCVC at all 5 propofol dose levels. Each regional SCVC was normalized to its own average across all 5 propofol doses and plotted into matrices (Fig. 5) based on the clustering results. Then one-way analysis of variance (ANOVA) was applied for each regional SCVC across all 5 propofol doses to test the dose-dependency.

Results

Physiological variables

Table 1 shows the means and standard deviations of the physiological parameters within 10 min after the start of each propofol dose. There were minor alterations in mean arterial blood pressure, heart rate, peripheral arterial oxygen saturation, and blood gas measurements after each change in propofol dose, but all were within the normal physiological range (Brammer et al., 1993). EEG waveforms, EEG band powers and behavioral scores were analyzed from stress testing experiments in non-paralyzed animals for the potential effects of gradient noise and head restraint at 20 and 40 mg/kg/h propofol doses. The results indicated no difference in the EEG and behavioral scores during the application of gradient noise or gradient noise with head restraint as compared to those during the noiseless free condition at either propofol dose (Fig. 2). Blood gas measurements at 20, 60, and 100 mg/kg/h propofol doses were performed in 6 additional rats under procedures and timeline of interventions identical to those in the functional imaging experiments. The obtained values were within physiological range (Supplementary Table 1).

Propofol-induced changes in electrocortical activity

The effect of increasing propofol dose on the EEG was characterized by a progression from desynchronized (low-amplitude, high-frequency) activity, to predominantly slow-wave activity, and finally to burst suppression at the lowest, middle, and highest doses, respectively. Multivariate

Table 1
Physiological parameter measurements taken within 10 min after the start of each propofol dose.

Propofol dose (mg/kg/h)	BP (mm Hg)	HR (bpm)	SPO_2 (%)	T °C
20	148 ± 22	315 ± 28	90 ± 5	37.2 ± 0.2
40	145 ± 23	320 ± 26	92 ± 8	37.5 ± 0.5
60	152 ± 25	301 ± 21	89 ± 5	37.4 ± 0.4
80	166 ± 20	332 ± 29	91 ± 4	37.5 ± 0.3
100	143 ± 20	317 ± 31	90 ± 6	36.9 ± 0.3

Mean ± SD. BP: mean arterial blood pressure; HR; heart rate; SPO_2: saturation of peripheral oxygen; T: temperature.

ANOVA revealed that delta ($P < 0.01$), theta ($P < 0.01$), alpha ($P < 0.01$), beta ($P < 0.005$), low-gamma ($P < 0.005$), and high-gamma ($P < 0.05$) differed as a function of propofol dose (Fig. 3). Post-hoc tests revealed that delta-band power was significantly augmented by 133 ± 42% as the propofol dose transitioned from 20 to 40 mg/kg/h ($P < 0.05$, Tukey–Kramer multiple comparison test). Theta, alpha, also decreased, but beta band power remained steady at both doses. Low and high-gamma powers were significantly suppressed by 38 ± 26 and 55 ± 4%, respectively, at 40 mg/kg/h compared with 20 mg/kg/h ($P < 0.05$, Tukey–Kramer multiple comparison test). At 40 mg/kg/h to 60 mg/kg/h propofol infusion rates, no significant change in power was observed at any of the investigated frequency bands. As propofol increased from 60 to 80 mg/kg/h, delta power was suppressed by 55 ± 5%, and returned to near baseline levels, when transitioning from 60 to 80 mg/kg/h ($P < 0.05$, Tukey–Kramer multiple comparison test). In addition, theta, alpha, and beta band powers were suppressed by 47 ± 7, 42 ± 9, and 66 ± 15%, respectively ($P < 0.05$). No changes in any of the five frequency band powers were observed between 80 and 100 mg/kg/h.

As an additional measure of the effect of propofol on the EEG, BSR was computed (Fig. 3 inset). Tukey–Kramer multiple comparison tests, after ANOVA, revealed that BSR was significantly higher at 80 mg/kg/h (0.515 ± 0.183) and 100 mg/kg/h (0.697 ± 0.166), when compared with 20 (0.031 ± 0.029), 40 (0.045 ± 0.051), and 60 mg/kg/h (0.110 ± 0.067) ($P < 0.05$).

Effect of propofol on whole brain functional connectivity

For visual inspection, significant FC maps were superimposed on the corresponding anatomical template and displayed for the selected seed ROIs (Fig. 1C). Fig. 1D shows the corresponding raw EEG traces at five propofol doses in one representative rat. The maps show widespread FC at 20 mg/kg/h dose with a relatively greater volume compared to that of other doses. When the propofol dose increased from 40 to 60 mg/kg/h, the FC area increased across all ROIs. At 80 mg/kg/h, FC showed partial recovery, but decreased again at 100 mg/kg/h, suggesting multiphasic modification with progressively deepening propofol anesthesia.

Illustrated in Figs. 4A and B are the relative (normalized to its own average across all 5 propofol doses) whole brain SCVC of each seed ROI in cortical and subcortical groups from all experiments. For most cortical seed ROIs, especially S1 and PtA, whole brain SCVC decreased, then recovered, and decreased again at increasing propofol dose. Subcortical ROIs, specifically NBM and mTH, displayed relatively stable whole brain SCVC.

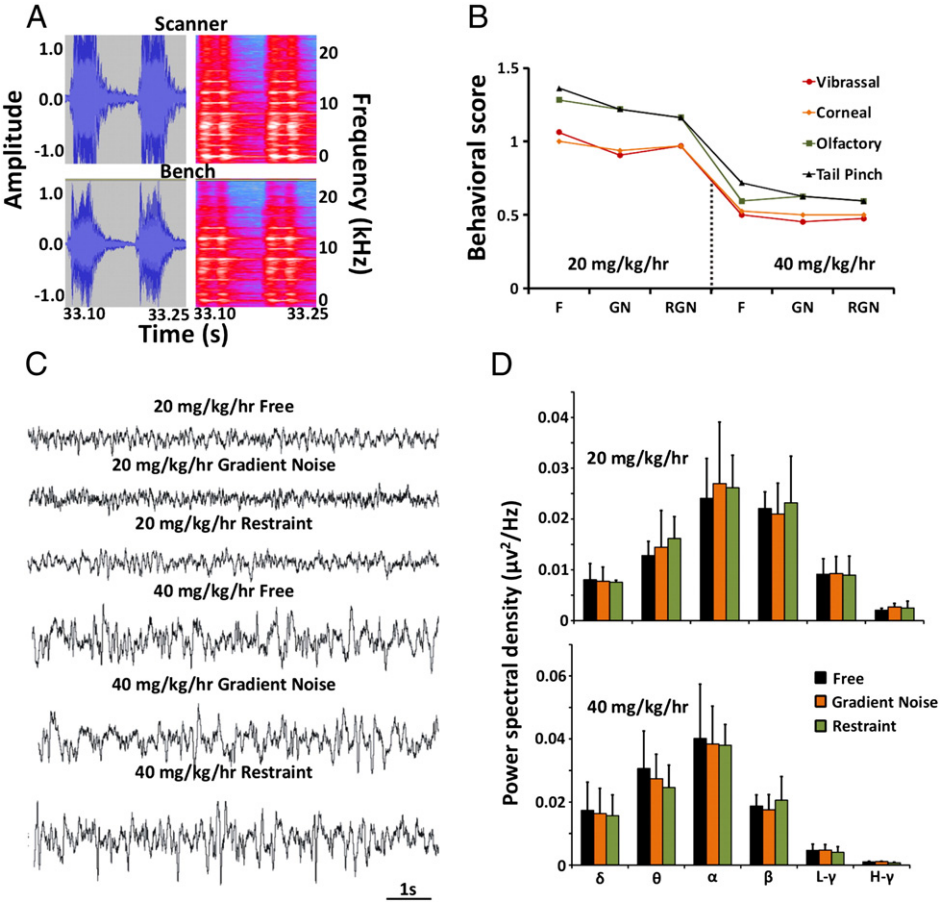

Fig. 2. Stress control. A. Comparison of recorded gradient noise waveforms and spectrograms (two beeps) in the scanner and on the bench; B. Behavioral test scores in noiseless free (F), gradient noise (GN) and restraint and GN (RGN) conditions at two propofol doses; C. EEG traces from a representative rat under each condition and both propofol doses. D. EEG band powers at the 20 and 40 mg/kg/h.

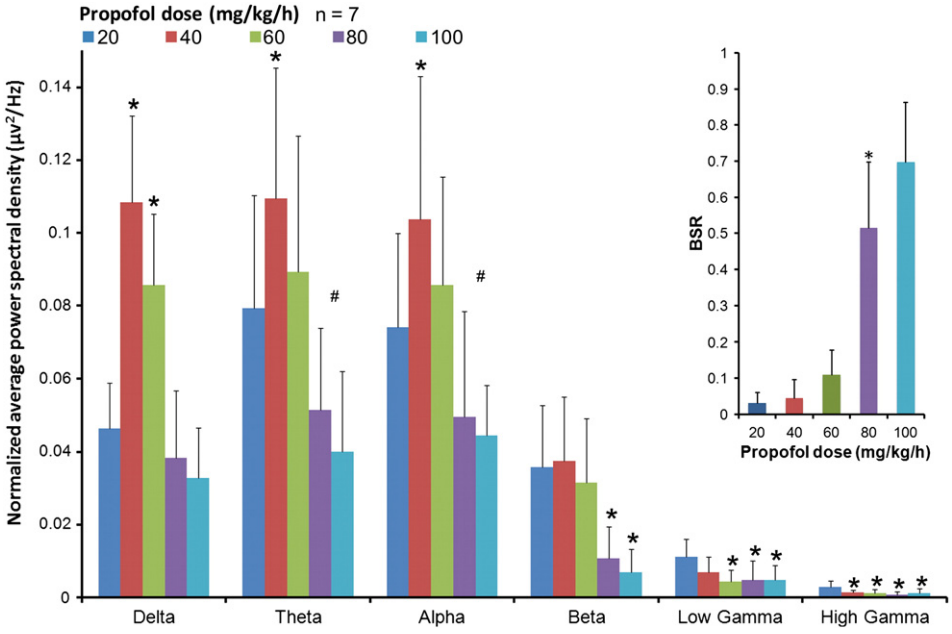

Fig. 3. Electroencephalogram power in five frequency bands at each propofol dose. Displayed are the normalized group means of EEG band power that differed as a function of propofol dose.*: $P < 0.05$ Tukey–Kramer multiple comparison test. Difference relative to the lowest dose (20 mg/kg/h). #: $P < 0.01$ Repeated measures ANOVA with planned comparison. Difference relative to the three lowest doses (20, 40, and 60 mg/kg/h). Burst suppression ratio (BSR) at each propofol dose are displayed in the insert. BSR remained stable 20, 40, and 60 mg/kg/h, respectively, but increased dramatically at 80 mg/kg/h. *$P < 0.05$ Tukey–Kramer multiple comparison test. Error bars are ± 1 SD; n = number of rats.

To determine if there were similarities among the networks in the manner they responded to increasing propofol dose, the changes of whole brain SCVC values for each seed ROI at the three lower propofol doses (20, 40, and 60 mg/kg/h) were subjected to K-mean clustering. We used the first three doses only because of their relevance to the change in conscious state and because they were free from EEG burst-suppression. The 12 seed ROIs were segregated into four clusters, two cortical (Ctx1 and Ctx2), and two subcortical (Sub1 and Sub2), as shown Fig. 4C. The ROIs in each cluster responded in a similar fashion to increasing propofol dose, but responses of the four clusters were distinct from one another. The average whole brain SCVC at each propofol dose for each cluster was displayed in Fig. 4D. In the first cortical cluster containing AC, M1, Retro and V1/V2, a significant decrease in the average voxel count was observed at 40 mg/kg/h, which remained relatively stable afterwards. In the second cortex cluster containing PtA and S1, the early reduction in whole brain SCVC was followed by a distinct increase at 60 mg/kg/h. The pattern of modifications was different in the subcortical clusters. For the first subcortical cluster (PnO, Hipp, and CPu), the whole brain SCVC progressively decreased until 60 mg/kg/h and recovered afterwards. For the second subcortical cluster (mTh, Hypo, and NBM), the whole brain SCVC remained relatively stable until an increase at 100 mg/kg/h.

Effect of propofol on regional functional connectivity

To investigate the region-to-region connectivity changes, the whole brain SCVC map was segmented into the 12 anatomical regions as delineated in Fig. 1B (target region) and the regional SCVC was measured for each seed ROI. To visualize the connectivity changes, the SCVC of each target region for each seed ROI was plotted as the relative voxel count in a matrix form (Fig. 5). At 20 mg/kg/h, the regional SCVC was relatively high for most brain region pairs, covering cortical to cortical (C–C), cortical to subcortical (C–S), subcortical to cortical (S–C), and subcortical to subcortical (S–S) connections. When the propofol dose was increased to 40 mg/kg/h, most region pairs decreased SCVC except for those pairs in the S–S quadrant of the matrix. A distinct quadrant boundary was identified at 60 mg/kg/h, when only the C–C connectivity rebounded, while the SCVC of almost all other region pairs decreased. Later, when the propofol dose was increased to 80 and 100 mg/kg/h, SCVC in the C–C quadrant decreased again, whereas the value recovered, especially at 100 mg/kg/h, in the other quadrants.

One-way repeated-measures ANOVA of the normalized regional SCVC values at the five propofol doses revealed a significant dependence on propofol dose for several regions (see Fig. 4, $P < 0.05$ FDR corrected). A particularly consistent effect of propofol was seen on the regional connectivity of Retro/S1. The connectivity of other regions affected was in the C–S and S–C quadrants, such as the Hipp, CPu, and NBM. For further statistical testing, the regional SCVC values in the four quadrants were pooled. All four quadrants showed a significant dependence on the propofol dose (repeated-measures ANOVA, $P < 0.000001$ FDR corrected). The means and 95% confidence intervals of the pooled regional SCVC at each propofol dose in each quadrant of the matrices in Fig. 4 are shown in Table 2. Significant reductions in regional SCVC from the 20 mg/kg/h dose were present at one or more propofol doses in all four quadrants.

Discussion

The goal of this study was to determine how propofol anesthesia alters intrinsic, resting-state functional connectivity in the rat brain. We found, to our knowledge for the first time, that progressively increasing depth of propofol anesthesia confers multiphasic, dose-dependent changes in functional connectivity and that these changes are substantially different in various cortical and subcortical networks.

General anesthetics cause a progressive and global decrease in neuronal activity (Hudetz et al., 2009), cerebral metabolism (Alkire et al., 1995, 1999; Cavazzuti et al., 1991; Dam et al., 1990) and cerebral blood flow (Fiset et al., 1999, 2005; Ogawa et al., 2003; Prielipp et al., 2002; Veselis et al., 1997). However, former rsfMRI studies in humans (Boveroux et al., 2010; Liu et al., 2012a; Mhuircheartaigh et al., 2010; Schroter et al., 2012; Schrouff et al., 2011; Stamatakis et al., 2010) and animals (Hutchison et al., 2010; Kannurpatti et al., 2008; Lu et al., 2007; Majeed et al., 2011; Pawela et al., 2009; Tu et al., 2011; Vincent et al., 2007; Williams et al., 2010; Zhao et al., 2008) found that during sedation or moderate depths of anesthesia brain functional connectivity may undergo complex changes with at least a partial

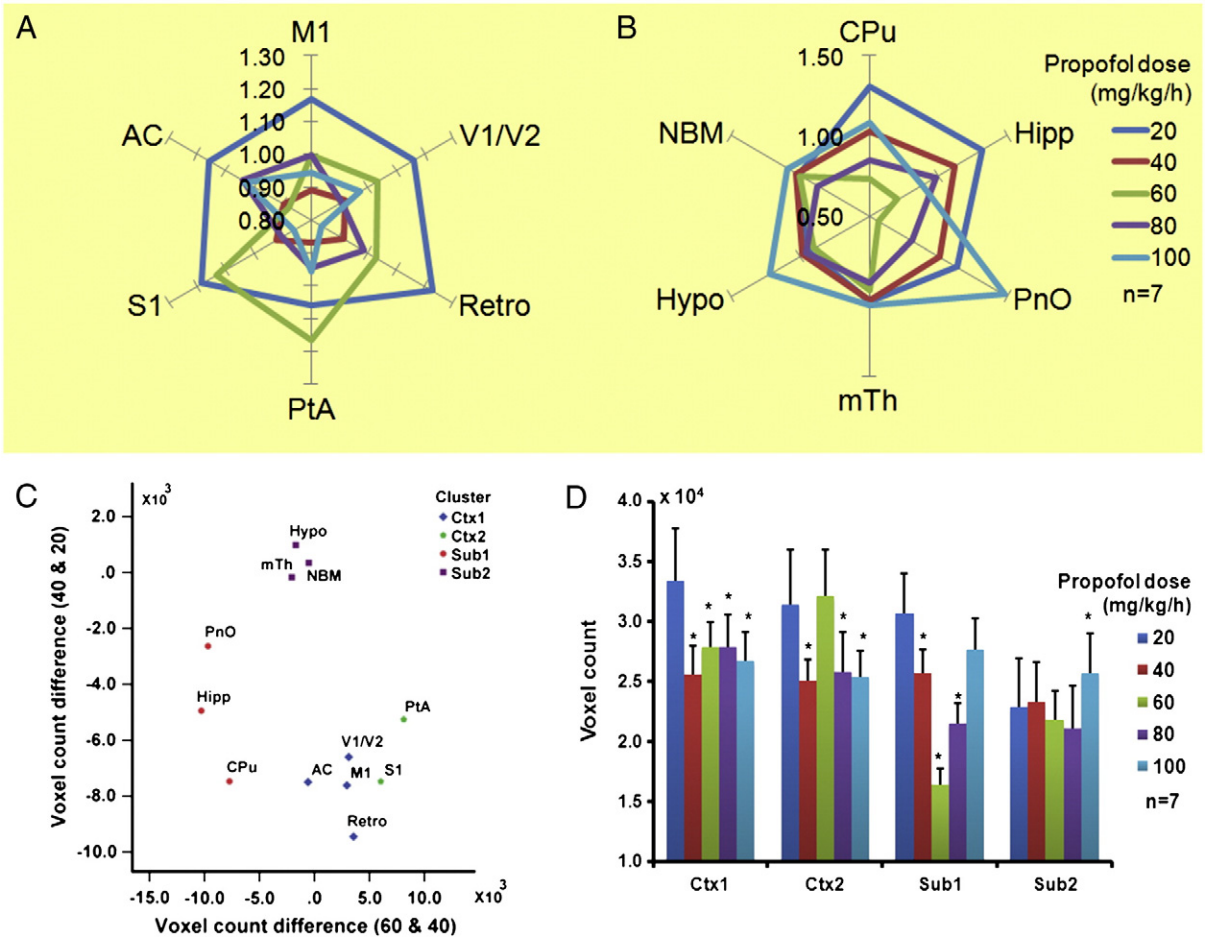

Fig. 4. Whole brain significantly connected voxel count (SCVC) and ROI clustering. A. Relative (normalized to its own average across 5 propofol doses) whole brain SCVC ($Z >= 0.5$) for cortical seed ROIs; B. Relative whole brain SCVC for subcortical seed ROIs; C. K-means clustering result using the whole brain SCVC change between 40 and 20 mg/kg/h propofol dose vs whole brain SCVC change between 60 and 40 mg/kg/h propofol dose; D. Cluster-averaged whole brain SCVC for each cluster of seed ROIs in C, * indicates *Student's t*-test significance from the 20 mg/kg/h values ($P < 0.05$). ROIs: anterior cingulate (AC), motor cortex (M1), primary sensory cortex (S1), parietal association cortex, motor cortex (M1), retrosplenium (Retro), visual cortex (V1/V2), hippocampuse (Hipp), caudate putamen (CPu), nucleus basalis of Meynert (NBM), medial thalamus (mTh), hypothalamus (Hypo), and oral part of the pontine reticular nucleus (PnO).

preservation of connectivity in specific networks. For example, during propofol anesthesia, functional connectivity between the putamen and thalamus was reduced, thalamocortical connectivity was preserved, and the connectivity between posterior cingulate cortex and sensorimotor cortices, pontine tegmentum and anterior thalamus was increased (Stamatakis et al., 2010). Fronto-parietal connectivity was partially decreased, whereas default-mode network connectivity was relatively unchanged (Boveroux et al., 2010; Stamatakis et al., 2010). The frontoparietal functional disconnection by propofol, as well as by inhalational anesthetics, has been confirmed by electroencephalographic studies (Boly et al., 2012b; Imas et al., 2005; Lee et al., 2009b).

Using the standard seed-based correlation followed by cluster analysis, we found two typical patterns of response to propofol in the cerebral cortex. The first response pattern was observed in regions that make up the so-called "default" network (anterior cingulate and retrosplenial cortex) as well as visual and motor regions. In humans, the default network presumably serves a self-referential function (Raichle et al., 2001; Vincent et al., 2008) and it was recently identified in rats (Liang et al., 2011; Lu et al., 2012; Upadhyay et al., 2011). The connectivity of these regions was quite sensitive to propofol in that it was already reduced at the second dose (40 mg/kg/h) and remained reduced at all the higher doses.

The second cortical response pattern occurred in a group of regions that consisted of the parietal association and primary somatosensory cortices. These regions are involved in the processing of multimodal sensory information, as well as bodily and spatial awareness (Kolb, 1990). The response of this group was similar to the first cortical group except that its functional connectivity transiently recovered at 60 mg/kg/h. The early decrease in the connectivity of the sensory, motor and parietal association cortices is consistent with the reduction in frontoparietal connectivity as previously indicated. The functional significance of the transient recovery at the third propofol dose is presently unclear. We speculate that it may be the result of subcortical disinhibition or of a homeostatic compensatory mechanism (Kaisti et al., 2003). Alternatively, it may indicate a second-order state transition typical to nonlinear systems (Hudetz et al., 2009; Steyn-Ross et al., 2001, 2003).

Two typical patterns were also seen in the subcortical connectivity response to propofol. In the first subcortical group (brainstem–hippocampus–caudate/putamen axis), functional connectivity decreased substantially at the two intermediate doses, but then recovered at the highest dose. The networks in this group are important for motor and cognitive functions, memory, and the modulation of pain. The largest decrease in connectivity was in the caudate–putamen, similar to that seen previously in humans (Martuzzi et al., 2010; Mhuircheartaigh et al., 2010).

Functional connectivity of the second subcortical group (medial thalamus, hypothalamus, and n. basalis of Meynert) was not reduced

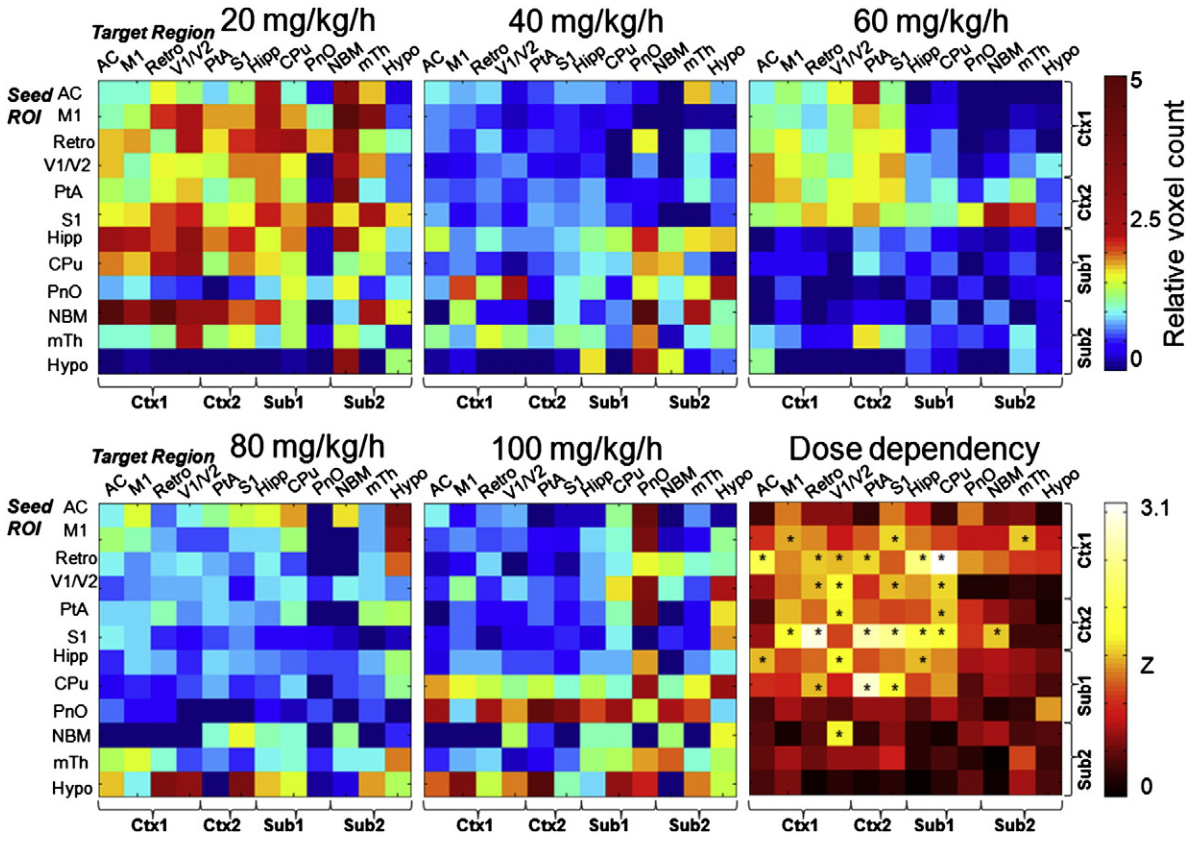

Fig. 5. Relative regional significantly connected voxel count (SCVC) for each seed ROI at each propofol dose level. Whole brain SCVC ($Z >= 0.5$) for each seed ROI (row) at each propofol dose level was segmented into each target region (column) and normalized to its own average across all 5 propofol doses and displayed according to the top right color bar. The bottom right panel shows the one-way ANOVA (propofol dose-dependency test) Z score (transformed from F values) for each cell of the previous 5 matrices, displayed according to the bottom right color bar; *Indicates FDR corrected significance for propofol dose dependency ($P < 0.05$). All ROIs are ordered based on the clustering results shown in Fig. 3C.

by propofol. The latter group is part of a network that regulates cortical arousal and sleep–wake states (Alkire et al., 2008; Jones, 2003; Laureys, 2005). The intralaminar and medial thalamic nuclei play important roles in enabling the conscious state (Alkire et al., 2000; Schiff, 2008; Schiff and Plum, 2000; Tononi, 2010). Pharmacological stimulation of the medial thalamus, hypothalamus and basal forebrain components can facilitate awakening from sleep and anesthesia (Alkire et al., 2007; Devor and Zalkind, 2001; Franks, 2008; Pillay et al., 2011; Reiner et al., 2007). Certain anesthetic agents may target components of these systems and the disruption of these pathways can lead to unconsciousness (Franks, 2008; Lu et al., 2008; Zecharia and Franks, 2009). The preservation of functional connectivity of these structures under propofol anesthesia is therefore surprising. It may suggest that propofol preferentially targets cortical rather than subcortical connectivity and its effects on state are not arousal-related. The preservation of thalamocortical functional connectivity is consistent with recent human (Mhuircheartaigh et al., 2010) and animal data (Silva et al., 2010). Of note is that our results concern the medial thalamus only and they do not inform about the possible connectivity changes of thalamic relay nuclei.

At the highest dose of propofol (100 mg/kg/h), we also observed a recovery of subcortical connectivity. This depth of anesthesia was characterized by EEG burst-suppression — a stereotypic, hypersynchronized state of the entire brain (Alkire et al., 2008; Tononi, 2004), accompanied by sensory hyperexcitability (Amzica, 2009; Hudetz, 2009; Hudetz and Imas, 2007; Kroeger and Amzica, 2007). Interestingly, the presence of burst-suppression did not alter cortical functional connectivity suggesting that the latter is of subcortical origin.

While the detailed reasons are not yet known, the observed multiphasic behavior in functional connectivity as reflected by both the SCVC (Fig. 5) and correlation strength (Supplementary Fig. 4) could be the result of dose-dependent sensitivity of various populations of excitatory and inhibitory receptors, specific types of neurons, pathways, and circuits in the brain. As the anesthetic dose is increased, different functional changes in circuitry are not unexpected. At behavioral level, four classical stages of general anesthesia are distinguished: induction (sedation), paradoxical excitation, surgical anesthesia, and deep anesthesia. Loss of consciousness occurs between the excitation phase and the surgical plane of anesthesia. Excitatory phase is commonly observed with propofol (Kuizenga et al., 2001) and may be associated with an

Table 2
The mean (95% confidence interval, CI) of relative significantly connected voxel count at each propofol dose level.

Propofol dose (mg/kg/h)	Ctx–Ctx mean (95%CI)	Ctx–Sub mean (95%CI)	Sub–Ctx mean (95%CI)	Sub–Sub mean (95%CI)
20	1.58 (1.52–1.65)	1.85 (1.65-2.05)	1.65 (1.43–1.87)	1.13 (0.96–1.29)
40	0.59 (0.52–0.66)*	0.49 (0.29–0.69)*	0.77 (0.55–1.00)*	1.33 (1.17–1.50)
60	1.47 (1.40–1.53)	0.60 (0.40–0.80)*	0.37 (0.15–0.59)*	0.35 (0.19–0.52)*
80	0.87 (0.80–0.93)*	0.87 (0.67–1.07)*	0.85 (0.63–1.07)*	0.77 (0.60–0.93) *
100	0.49 (0.43–0.56)*	1.19 (0.99–1.39)*	1.35 (1.13–1.58)	1.42 (1.26–1.59)

Results shown are pooled data from each quadrant of the matrices in Fig. 4. Ctx: Cortical; Sub: Subcortical.
* Indicates significance ($P < 0.05$) of the Tukey's post-hoc test comparing with that of the 20 mg/kg/h dose level.

increase in connectivity in certain brain regions. In fact, anesthetic agents have been found to affect distinct regions of the brain in a differential manner, rather than by a global suppression activity to the same degree across all regions (Boly et al., 2012a; Hudetz, 2012; Nallasamy and Tsao, 2011).

A recent important study by Liu and colleagues (Liu et al., 2012b) examined BOLD functional connectivity in the somatosensory cortex of unconscious rats anesthetized with various doses of isoflurane from 1.0% to 1.8%. They found that at increasing depth of anesthesia, spatially specific functional connectivity was masked by an independent added effect of globally synchronized activity associated with the development of EEG burst suppression. We did not find such an increase in global cortical connectivity under burst-suppression conditions with propofol; connectivity increases were limited to subcortical networks. The difference may be due to the propensity of isoflurane to cause an increase in cerebral blood flow (Lee et al., 1994), which may augment cortical BOLD signals and functional connectivity. It is important to note that we chose not to regress out the global BOLD signal because we thought that it may contain valuable information about brain state. The benefits and drawbacks of global signal regression have been debated (Chen et al., 2012; Murphy et al., 2009; Saad et al., 2012). However, anesthetic-induced changes in the global signal could influence the overall level of SCVC (Liu et al., 2011) To examine this issue, we compared SCVC changes with and without global signal regression and found that it did not abolish the multiphasic changes we found in SCVC (as in Supplementary Fig. 3) although it decreased the overall SCVC numbers in most regions. The quality of our data was good, overall, with a high signal to noise ratio (SNR = 90–110 for NBM and mTh, 85–100 for the deepest region Hypo) and we concluded that global signal regression in our study was not necessary (Chen et al., 2012). Additional differences between the studies by Liu (Liu et al., 2012b) and ours were that we assessed whole brain connectivity, measured EEG simultaneously with fMRI, and our experimental protocol also included lower levels of anesthesia corresponding to conscious sedation. The general reduction in cortical functional connectivity due to propofol appears to be more consistent with that observed with alpha-chloralose (Lu et al., 2007), although only propofol revealed regionally specific multiphasic changes as a function of anesthetic dose. The deepest level of anesthesia was associated with delta EEG in Lu's study.

Recent studies found that propofol may change the shape of the hemodynamic response function due to a decrease in baseline cerebral blood flow (Liu et al., 2013; Masamoto and Kanno, 2012). In a group of six additional rats we examined the changes in regional cerebral blood flow (rCBF) measured with dynamic susceptibility contrast (Pincus et al., 1996) scans (Supplementary Methods and Supplementary Fig. 2). There was a small decrease of 8 ± 3% ($P > 0.05$) in cortical (mainly frontal) and only 5 ± 2% ($P > 0.05$) in subcortical regions in rCBF when increasing propofol from 20 to 60 mg/kg/h. This is consistent with the generally small reduction in rCBF previously observed with propofol (Fiset et al., 1999). rCBF decreased further when propofol was increased to 100 mg/kg/h; rCBF decreased 20 ± 6% ($P < 0.05$) in cortical and 14 ± 5% ($P < 0.05$) in subcortical regions. For all ROIS, a general dose-dependent decrease in rCBF was observed (repeated measure ANOVA, $P < 0.001$) from propofol doses 20 to 60 and to 100 mg/kg/h. Changes in individual ROIs were only significant (post-hoc Turkey–Kramer, $P < 0.05$) at 100 mg/kg/h in the anterior cingulate (AC) and in a few subcortical regions (CPu, PnO, NBM, mTh). These rCBF changes differed from the multiphasic changes in connectivity shown earlier. In addition, the spatial pattern of rCBF reduction differed from that of the change in SCVC that were found both increasing and decreasing in various brain regions and propofol doses (particularly at 60 and 100 mg/kg/h). Although a modulation of connectivity patterns by the propofol-induced reductions in rCBF cannot be totally excluded, it is unlikely that those would be a major source of the multiphasic differential changes observed in SCVC. Because most anesthetic agents tend to dilate the cerebral vasculature while neurovascular coupling is preserved (Franceschini et al., 2010), the observed reduction in rCBF is most likely due to an overall reduction in neuronal activity as opposed to a direct cerebrovascular effect of propofol. Consequently, correlated spontaneous BOLD signal fluctuations should be driven by neuronal sources under various depths of anesthesia.

Functional connectivity and the neuronal mechanism of anesthesia

The principal goal of several recent functional imaging studies in humans has been to discover the putative neural correlate of anesthetic-induced loss and return of consciousness (Boly, 2011; Heine et al., 2012; Hudetz, 2012). General anesthetic agents produce not only unconsciousness but also areflexia, analgesia and amnesia. Areflexia to nociceptive stimuli has been ascribed to an anesthetic suppression of the excitability of spinal cord neurons (Antognini et al., 2007; Rampil and King, 1996), whereas amnesia and hypnosis (loss of consciousness) are associated with supraspinal effects (Alkire et al., 2008; Veselis, 2001). A principled and accurate determination of the neuronal mechanisms of hypnosis is hindered by the lack of objective definition and tool for assessment of the state of consciousness. This limitation is especially obvious in animals, where only indirect, behavioral indices of state are available. Based on the equivalence of corresponding anesthetic doses that produce loss of voluntary responsiveness in humans (Franks, 2008), the loss of righting reflex has been widely used as a surrogate index of unconsciousness in rodents. As guided by prior bench experiments and other studies in the literature (Tung et al., 2002), the critical dose of propofol that produces loss of righting reflex is obtained at a steady-state infusion rate of approximately 40 mg/kg/h. Therefore, this dose has been taken as a putative threshold for loss of consciousness in rats. The appearance of a synchronized EEG pattern characteristic to unconscious states in general provided additional confidence to this choice.

The impact of findings of rsfMRI studies including those from the present investigation hinges on several factors. First, both fMRI and rsfMRI are indirect measures of neuronal activity, thus an extrapolation of the results to neural mechanisms requires caution. Cerebrovascular effects of anesthetics that may influence BOLD imaging are well known, although propofol at a hypnotic dose has been found to exert a minor cerebrovascular effect (Fiset et al., 1999). Recent investigations have provided evidence for a reliable correlation between resting-state BOLD functional connectivity and neuronal activity (Liu et al., 2011, 2012b; Lu et al., 2007; Scheeringa et al., 2012; Scholvinck et al., 2010; Shmuel and Leopold, 2008; Sumiyoshi et al., 2012). Nevertheless, the observed changes in BOLD functional connectivity may be interpreted with some caution. While a decrease in functional connectivity may suggest uncoupling of brain regions, an increase in functional connectivity may also indicate reduced neuronal communication due to hypersynchrony, which is a stereotypic information-deprived form of activity (Alkire et al., 2008; Ferrarelli et al., 2010; Schrouff et al., 2011; Stamatakis et al., 2010).

A direct assessment of functional connectivity from neuroelectric signals simultaneously with rsfMRI was not technically feasible in our rat experiments. The combination of novel electrophysiological and rsfMRI techniques in rodents (Mishra et al., 2011; Ogawa et al., 2000; Pan et al., 2011) and humans (Hill et al., 2012; Mankinen et al., 2011) may provide the necessary further insight into the nature of neuronal connectivity associated with BOLD functional connectivity. Changes in cortical connectivity (Lee et al., 2009a) and global coherence (Cimenser et al., 2011) derived from multisite EEG recordings during propofol anesthesia are now actively studied in human subjects.

Finally, future investigations will have to address the question whether the observed changes in functional connectivity may be causally related to the observed changes in the state of consciousness. The observed reductions in connectivity are partial and their impact on neuronal and cognitive functions is unclear. In particular, what magnitude of change in functional connectivity would be necessary and sufficient to account

for the loss of cognition and consciousness? It is also unclear if cognitive functions, memory and consciousness are reduced by anesthetics gradually or abruptly — an issue that has proponents on both sides (Alkire et al., 2008; Hudetz and Pearce, 2009; Steyn-Ross et al., 2001; Veselis et al., 2001). The answer would clearly influence the types of change in connectivity that would qualify as the neural correlates of anesthetic state transitions

Conclusions

Graded levels of propofol anesthesia in rats alter the BOLD functional connectivity of distinct regional networks in a differential and multiphasic manner. Cortical connectivity is suppressed before subcortical connectivity; the cortical effects are evident at a critical dose of propofol that corresponds to the presumed loss of consciousness. Subcortical but not cortical connectivity recovers in deep anesthesia associated with EEG burst suppression suggesting the role of subcortical ascending modulation in producing cortical hyperexcitability. Together, the results suggest specific alterations in network functional connectivity that may be associated with the anesthetic modulation of state of consciousness in the rat brain.

Supplementary data to this article can be found online at http://dx.doi.org/10.1016/j.neuroimage.2013.07.003.

Acknowledgments

Research reported in this publication was supported by the National Institute of General Medical Sciences of the National Institutes of Health under Award Number R01-GM056398 (to AGH) and by Pre-doctoral Graduate Assistance in Areas of National Need (GAANN) fellowship from the Department of Education, Washington, DC (to JAV). The content is solely the responsibility of the authors and does not necessarily represent the official views of the National Institutes of Health.

Conflict of interest

The authors of this manuscript disclosed no conflict of interest.

References

Alkire, M.T., Haier, R.J., Barker, S.J., Shah, N.K., Wu, J.C., Kao, Y.J., 1995. Cerebral metabolism during propofol anesthesia in humans studied with positron emission tomography. Anesthesiology 82, 393–403 (discussion 327A).
Alkire, M.T., Pomfrett, C.J., Haier, R.J., Gianzero, M.V., Chan, C.M., Jacobsen, B.P., Fallon, J.H., 1999. Functional brain imaging during anesthesia in humans: effects of halothane on global and regional cerebral glucose metabolism. Anesthesiology 90, 701–709.
Alkire, M.T., Haier, R.J., Fallon, J.H., 2000. Toward a unified theory of narcosis: brain imaging evidence for a thalamocortical switch as the neurophysiologic basis of anesthetic-induced unconsciousness. Conscious. Cogn. 9, 370–386.
Alkire, M.T., McReynolds, J.R., Hahn, E.L., Trivedi, A.N., 2007. Thalamic microinjection of nicotine reverses sevoflurane-induced loss of righting reflex in the rat. Anesthesiology 107, 264–272.
Alkire, M., Hudetz, A., Tononi, G., 2008. Consciousness and anesthesia. Science 322, 876–880.
Amzica, F., 2009. Basic physiology of burst-suppression. Epilepsia 50 (Suppl. 12), 38–39.
Antognini, J.F., Atherley, R.J., Dutton, R.C., Laster, M.J., Eger II, E.I., Carstens, E., 2007. The excitatory and inhibitory effects of nitrous oxide on spinal neuronal responses to noxious stimulation. Anesth. Analg. 104, 829–835.
Biswal, B., Yetkin, F.Z., Haughton, V.M., Hyde, J.S., 1995. Functional connectivity in the motor cortex of resting human brain using echo-planar MRI. Magn. Reson. Imaging 34, 537–541.
Boly, M., 2011. Measuring the fading consciousness in the human brain. Curr. Opin. Neurol. 24, 394–400.
Boly, M., Massimini, M., Garrido, M.I., Gosseries, O., Noirhomme, Q., Laureys, S., Soddu, A., 2012a. Brain connectivity in disorders of consciousness. Brain Connect. 2, 1–10.
Boly, M., Moran, R., Murphy, M., Boveroux, P., Bruno, M.A., Noirhomme, Q., Ledoux, D., Bonhomme, V., Brichant, J.F., Tononi, G., Laureys, S., Friston, K., 2012b. Connectivity changes underlying spectral EEG changes during propofol-induced loss of consciousness. J. Neurosci. 32, 7082–7090.
Boveroux, P., Vanhaudenhuyse, A., Bruno, M.A., Noirhomme, Q., Lauwick, S., Luxen, A., Degueldre, C., Plenevaux, A., Schnakers, C., Phillips, C., Brichant, J.F., Bonhomme, V., Maquet, P., Greicius, M.D., Laureys, S., Boly, M., 2010. Breakdown of within- and between-network resting state functional magnetic resonance imaging connectivity during propofol-induced loss of consciousness. Anesthesiology 113, 1038–1053.
Brammer, A., West, C.D., Allen, S.L., 1993. A comparison of propofol with other injectable anaesthetics in a rat model for measuring cardiovascular parameters. Lab. Anim. 27, 250–257.
Cavazzuti, M., Porro, C.A., Barbieri, A., Galetti, A., 1991. Brain and spinal cord metabolic activity during propofol anaesthesia. Br. J. Anaesth. 66, 490–495.
Chen, G., Chen, G., Xie, C., Ward, B.D., Li, W., Antuono, P., Li, S.J., 2012. A method to determine the necessity for global signal regression in resting-state fMRI studies. Magn. Reson. Med. 68, 1828–1835.
Cimenser, A., Purdon, P.L., Pierce, E.T., Walsh, J.L., Salazar-Gomez, A.F., Harrell, P.G., Tavares-Stoeckel, C., Habeeb, K., Brown, E.N., 2011. Tracking brain states under general anesthesia by using global coherence analysis. Proc. Natl. Acad. Sci. U. S. A. 108, 8832–8837.
Dam, M., Ori, C., Pizzolato, G., Ricchieri, G.L., Pellegrini, A., Giron, G.P., Battistin, L., 1990. The effects of propofol anesthesia on local cerebral glucose utilization in the rat. Anesthesiology 73, 499–505.
Dawson, D.A., Cha, K., Lewis, L.B., Mendola, J.D., Shmuel, A., 2012. Evaluation and calibration of functional network modeling methods based on known anatomical connections. NeuroImage.
Dean, P., 1990. Sensory cortex: visual perceptual functions. In: Kolb, B., Tees, R.C. (Eds.), The Cerebral Cortex of the Rat. MIT Press, Cambridge, pp. 275–307.
Devor, M., Zalkind, V., 2001. Reversible analgesia, atonia, and loss of consciousness on bilateral intracerebral microinjection of pentobarbital. Pain 94, 101–112.
Duyn, J., 2011. Spontaneous fMRI activity during resting wakefulness and sleep. Prog. Brain Res. 193, 295–305.
Erchova, I.A., Lebedev, M.A., Diamond, M.E., 2002. Somatosensory cortical neuronal population activity across states of anaesthesia. Eur. J. Neurosci. 15, 744–752.
Ferrarelli, F., Massimini, M., Sarasso, S., Casali, A., Riedner, B.A., Angelini, G., Tononi, G., Pearce, R.A., 2010. Breakdown in cortical effective connectivity during midazolam-induced loss of consciousness. Proc. Natl. Acad. Sci. U. S. A. 107, 2681–2686.
Fiset, P., Paus, T., Daloze, T., Plourde, G., Meuret, P., Bonhomme, V., Hajj-Ali, N., Backman, S.B., Evans, A.C., 1999. Brain mechanisms of propofol-induced loss of consciousness in humans: a positron emission tomographic study. J. Neurosci. 19, 5506–5513.
Fiset, P., Plourde, G., Backman, S.B., 2005. Brain imaging in research on anesthetic mechanisms: studies with propofol. Prog. Brain Res. 150, 245–250.
Franceschini, M.A., Radhakrishnan, H., Thakur, K., Wu, W., Ruvinskaya, S., Carp, S., Boas, D.A., 2010. The effect of different anesthetics on neurovascular coupling. NeuroImage 51, 1367–1377.
Franks, N.P., 2008. General anaesthesia: from molecular targets to neuronal pathways of sleep and arousal. Nat. Rev. Neurosci. 9, 370–386.
Gusnard, D.A., Raichle, M.E., 2001. Searching for a baseline: functional imaging and the resting human brain. Nat. Rev. Neurosci. 2, 685–694.
Heine, L., Soddu, A., Gomez, F., Vanhaudenhuyse, A., Tshibanda, L., Thonnard, M., Charland-Verville, V., Kirsch, M., Laureys, S., Demertzi, A., 2012. Resting state networks and consciousness: alterations of multiple resting state network connectivity in physiological, pharmacological, and pathological consciousness states. Front. Psychol. 3, 295.
Hill, N.J., Gupta, D., Brunner, P., Gunduz, A., Adamo, M.A., Ritaccio, A., Schalk, G., 2012. Recording human electrocorticographic (ECoG) signals for neuroscientific research and real-time functional cortical mapping. J. Vis. Exp.
Hudetz, A.G., 2009. Feedback suppression in anesthesia. Is it reversible? Conscious. Cogn. 18, 1079–1081.
Hudetz, A.G., 2012. General anesthesia and human brain connectivity. Brain Connect.
Hudetz, A.G., Imas, O.A., 2007. Burst activation of the cerebral cortex by flash stimuli during isoflurane anesthesia in rats. Anesthesiology 107, 983–991.
Hudetz, A.G., Pearce, R.A. (Eds.), 2009. Suppressing the Mind: Anesthetic Modulation of Memory and Consciousness, 1st ed. Humana Press, New York.
Hudetz, A.G., Vizuete, J.A., Imas, O.A., 2009. Desflurane selectively suppresses long-latency cortical neuronal response to flash in the rat. Anesthesiology 111, 231–239.
Hutchison, R.M., Mirsattari, S.M., Jones, C.K., Gati, J.S., Leung, L.S., 2010. Functional networks in the anesthetized rat brain revealed by independent component analysis of resting-state FMRI. J. Neurophysiol. 103, 3398–3406.
Imas, O.A., Ropella, K.M., Ward, B.D., Wood, J.D., Hudetz, A.G., 2005. Volatile anesthetics enhance flash-induced gamma oscillations in rat visual cortex. Anesthesiology 102, 937–947.
Jones, B., 2003. Arousal systems. Front. Biosci. 8, s438–s451.
Jugovac, I., Imas, O., Hudetz, A.G., 2006. Supraspinal anesthesia: behavioral and electroencephalographic effects of intracerebroventricularly infused pentobarbital, propofol, fentanyl, and midazolam. Anesthesiology 105, 764–778.
Kaisti, K.K., Langsjo, J.W., Aalto, S., Oikonen, V., Sipila, H., Teras, M., Hinkka, S., Metsahonkala, L., Scheinin, H., 2003. Effects of sevoflurane, propofol, and adjunct nitrous oxide on regional cerebral blood flow, oxygen consumption, and blood volume in humans. Anesthesiology 99, 603–613.
Kalthoff, D., Seehafer, J.U., Po, C., Wiedermann, D., Hoehn, M., 2011. Functional connectivity in the rat at 11.7 T: impact of physiological noise in resting state fMRI. NeuroImage 54, 2828–2839.
Kannurpatti, S.S., Biswal, B.B., Kim, Y.R., Rosen, B.R., 2008. Spatio-temporal characteristics of low-frequency BOLD signal fluctuations in isoflurane-anesthetized rat brain. NeuroImage 40, 1738–1747.
Keilholz, S., Magnuson, M.E., Pan, W.J., Willis, M., Thompson, G., 2012. Dynamic properties of functional connectivity in the rodent. Brain Connect.
Kolb, B., 1990. Posterior parietal and temporal association. In: Kolb, B., Tees, R.C. (Eds.), The Cerebral Cortex of the Rat. MIT Press, Cambridge, pp. 459–471.
Kroeger, D., Amzica, F., 2007. Hypersensitivity of the anesthesia-induced comatose brain. J. Neurosci. 27, 10597–10607.
Kuizenga, K., Wierda, J.M., Kalkman, C.J., 2001. Biphasic EEG changes in relation to loss of consciousness during induction with thiopental, propofol, etomidate, midazolam or sevoflurane. Br. J. Anaesth. 86, 354–360.

Laureys, S., 2005. The neural correlate of (un)awareness: lessons from the vegetative state. Trends Cogn. Sci. 9, 556–559.
Lee, J.G., Hudetz, A.G., Smith, J.J., Hillard, C.J., Bosnjak, Z.J., Kampine, J.P., 1994. The effects of halothane and isoflurane on cerebrocortical microcirculation and autoregulation as assessed by laser-Doppler flowmetry. Anesth. Analg. 79, 58–65.
Lee, U., Kim, S., Noh, G.J., Choi, B.M., Hwang, E., Mashour, G.A., 2009a. The directionality and functional organization of frontoparietal connectivity during consciousness and anesthesia in humans. Conscious. Cogn. 18, 1069–1078.
Lee, U., Mashour, G.A., Kim, S., Noh, G.J., Choi, B.M., 2009b. Propofol induction reduces the capacity for neural information integration: implications for the mechanism of consciousness and general anesthesia. Conscious. Cogn. 18, 56–64.
Liang, Z., King, J., Zhang, N., 2011. Uncovering intrinsic connectional architecture of functional networks in awake rat brain. J. Neurosci. 31, 3776–3783.
Liu, X., Zhu, X.H., Zhang, Y., Chen, W., 2011. Neural origin of spontaneous hemodynamic fluctuations in rats under burst-suppression anesthesia condition. Cereb. Cortex 21, 374–384.
Liu, X., Lauer, K.K., Ward, B.D., Rao, S.M., Li, S.J., Hudetz, A.G., 2012a. Propofol disrupts functional interactions between sensory and high-order processing of auditory verbal memory. Hum. Brain Mapp. 33, 2487–2498.
Liu, X., Zhu, X.H., Zhang, Y., Chen, W., 2012b. The change of functional connectivity specificity in rats under various anesthesia levels and its neural origin. Brain Topogr.
Liu, J.V., Hirano, Y., Nascimento, G.C., Stefanovic, B., Leopold, D.A., Silva, A.C., 2013. fMRI in the awake marmoset: somatosensory-evoked responses, functional connectivity, and comparison with propofol anesthesia. NeuroImage.
Lu, H., Zuo, Y., Gu, H., Waltz, J.A., Zhan, W., Scholl, C.A., Rea, W., Yang, Y., Stein, E.A., 2007. Synchronized delta oscillations correlate with the resting-state functional MRI signal. Proc. Natl. Acad. Sci. U. S. A. 104, 18265–18269.
Lu, J., Nelson, L.E., Franks, N., Maze, M., Chamberlin, N.L., Saper, C.B., 2008. Role of endogenous sleep–wake and analgesic systems in anesthesia. J. Comp. Neurol. 508, 648–662.
Lu, H., Zou, Q., Gu, H., Raichle, M.E., Stein, E.A., Yang, Y., 2012. Rat brains also have a default mode network. Proc. Natl. Acad. Sci. U. S. A. 109, 3979–3984.
Ma, J., Shen, B., Stewart, L.S., Herrick, I.A., Leung, L.S., 2002. The septohippocampal system participates in general anesthesia. J. Neurosci. 22, RC200.
Majeed, W., Magnuson, M., Hasenkamp, W., Schwarb, H., Schumacher, E.H., Barsalou, L., Keilholz, S.D., 2011. Spatiotemporal dynamics of low frequency BOLD fluctuations in rats and humans. NeuroImage 54, 1140–1150.
Mankinen, K., Long, X.Y., Paakki, J.J., Harila, M., Rytky, S., Tervonen, O., Nikkinen, J., Starck, T., Remes, J., Rantala, H., Zang, Y.F., Kiviniemi, V., 2011. Alterations in regional homogeneity of baseline brain activity in pediatric temporal lobe epilepsy. Brain Res. 1373, 221–229.
Mantini, D., Gerits, A., Nelissen, K., Durand, J.B., Joly, O., Simone, L., Sawamura, H., Wardak, C., Orban, G.A., Buckner, R.L., Vanduffel, W., 2011. Default mode of brain function in monkeys. J. Neurosci. 31, 12954–12962.
Martuzzi, R., Ramani, R., Qiu, M., Rajeevan, N., Constable, R.T., 2010. Functional connectivity and alterations in baseline brain state in humans. NeuroImage 49, 823–834.
Masamoto, K., Kanno, I., 2012. Anesthesia and the quantitative evaluation of neurovascular coupling. J. Cereb. Blood Flow Metab. 32, 1233–1247.
Mhuircheartaigh, R.N., Rosenorn-Lanng, D., Wise, R., Jbabdi, S., Rogers, R., Tracey, I., 2010. Cortical and subcortical connectivity changes during decreasing levels of consciousness in humans: a functional magnetic resonance imaging study using propofol. J. Neurosci. 30, 9095–9102.
Mishra, A.M., Ellens, D.J., Schridde, U., Motelow, J.E., Purcaro, M.J., DeSalvo, M.N., Enev, M., Sanganahalli, B.G., Hyder, F., Blumenfeld, H., 2011. Where fMRI and electrophysiology agree to disagree: corticothalamic and striatal activity patterns in the WAG/Rij rat. J. Neurosci. 31, 15053–15064.
Murphy, K., Birn, R.M., Handwerker, D.A., Jones, T.B., Bandettini, P.A., 2009. The impact of global signal regression on resting state correlations: are anti-correlated networks introduced? NeuroImage 44, 893–905.
Nallasamy, N., Tsao, D.Y., 2011. Functional connectivity in the brain: effects of anesthesia. Neuroscientist 17, 94–106.
Ogawa, S., Lee, T.M., Stepnoski, R., Chen, W., Zhu, X.H., Ugurbil, K., 2000. An approach to probe some neural systems interaction by functional MRI at neural time scale down to milliseconds. Proc. Natl. Acad. Sci. U. S. A. 97, 11026–11031.
Ogawa, K., Uema, T., Motohashi, N., Nishikawa, M., Takano, H., Hiroki, M., Imabayashi, E., Ohnishi, T., Inoue, T., Takayama, Y., Takeda, M., Matsuda, H., Andoh, T., Yamada, Y., 2003. Neural mechanism of propofol anesthesia in severe depression: a positron emission tomographic study. Anesthesiology 98, 1101–1111.
Pan, W.J., Thompson, G., Magnuson, M., Majeed, W., Jaeger, D., Keilholz, S., 2011. Broadband local field potentials correlate with spontaneous fluctuations in functional magnetic resonance imaging signals in the rat somatosensory cortex under isoflurane anesthesia. Brain Connect. 1, 119–131.
Pawela, C.P., Biswal, B.B., Cho, Y.R., Kao, D.S., Li, R., Jones, S.R., Schulte, M.L., Matloub, H.S., Hudetz, A.G., Hyde, J.S., 2008. Resting-state functional connectivity of the rat brain. Magn. Reson. Med. 59, 1021–1029.
Pawela, C.P., Biswal, B.B., Hudetz, A.G., Schulte, M.L., Li, R., Jones, S.R., Cho, Y.R., Matloub, H.S., Hyde, J.S., 2009. A protocol for use of medetomidine anesthesia in rats for extended studies using task-induced BOLD contrast and resting-state functional connectivity. NeuroImage 46, 1137–1147.
Pillay, S., Vizuete, J.A., McCallum, J.B., Hudetz, A.G., 2011. Norepinephrine infusion into nucleus basalis elicits microarousal in desflurane-anesthetized rats. Anesthesiology 115, 733–742.
Pincus, S.M., Mulligan, T., Iranmanesh, A., Gheorghiu, S., Godschalk, M., Veldhuis, J.D., 1996. Older males secrete luteinizing hormone and testosterone more irregularly, and jointly more asynchronously, than younger males. Proc. Natl. Acad. Sci. U. S. A. 93, 14100–14105.
Power, J.D., Cohen, A.L., Nelson, S.M., Wig, G.S., Barnes, K.A., Church, J.A., Vogel, A.C., Laumann, T.O., Miezin, F.M., Schlaggar, B.L., Petersen, S.E., 2011. Functional network organization of the human brain. Neuron 72, 665–678.
Prielipp, R.C., Wall, M.H., Tobin, J.R., Groban, L., Cannon, M.A., Fahey, F.H., Gage, H.D., Stump, D.A., James, R.L., Bennett, J., Butterworth, J., 2002. Dexmedetomidine-induced sedation in volunteers decreases regional and global cerebral blood flow. Anesth. Analg. 95, 1052–1059 (table of contents).
Raichle, M.E., MacLeod, A.M., Snyder, A.Z., Powers, W.J., Gusnard, D.A., Shulman, G.L., 2001. A default mode of brain function. Proc. Natl. Acad. Sci. U. S. A. 98, 676–682.
Rampil, I.J., King, B.S., 1996. Volatile anesthetics depress spinal motor neurons. Anesthesiology 85, 129–134.
Reiner, K., Sukhotinsky, I., Devor, M., 2007. Mesopontine tegmental anesthesia area projects independently to the rostromedial medulla and to the spinal cord. Neuroscience 146, 1355–1370.
Saad, Z.S., Gotts, S.J., Murphy, K., Chen, G., Jo, H.J., Martin, A., Cox, R.W., 2012. Trouble at rest: how correlation patterns and group differences become distorted after global signal regression. Brain Connect. 2, 25–32.
Scheeringa, R., Petersson, K.M., Kleinschmidt, A., Jensen, O., Bastiaansen, M.C., 2012. EEG alpha power modulation of FMRI resting-state connectivity. Brain Connect. 2, 254–264.
Schiff, N.D., 2008. Central thalamic contributions to arousal regulation and neurological disorders of consciousness. Ann. N. Y. Acad. Sci. 1129, 105–118.
Schiff, N.D., Plum, F., 2000. The role of arousal and "gating" systems in the neurology of impaired consciousness. J. Clin. Neurophysiol. 17, 438–452.
Scholvinck, M.L., Maier, A., Ye, F.Q., Duyn, J.H., Leopold, D.A., 2010. Neural basis of global resting-state fMRI activity. Proc. Natl. Acad. Sci. U. S. A. 107, 10238–10243.
Schroter, M.S., Spoormaker, V.I., Schorer, A., Wohlschlager, A., Czisch, M., Kochs, E.F., Zimmer, C., Hemmer, B., Schneider, G., Jordan, D., Ilg, R., 2012. Spatiotemporal reconfiguration of large-scale brain functional networks during propofol-induced loss of consciousness. J. Neurosci. 32, 12832–12840.
Schrouff, J., Perlbarg, V., Boly, M., Marrelec, G., Boveroux, P., Vanhaudenhuyse, A., Bruno, M.A., Laureys, S., Phillips, C., Pelegrini-Issac, M., Maquet, P., Benali, H., 2011. Brain functional integration decreases during propofol-induced loss of consciousness. NeuroImage 57, 198–205.
Shmuel, A., Leopold, D.A., 2008. Neuronal correlates of spontaneous fluctuations in fMRI signals in monkey visual cortex: Implications for functional connectivity at rest. Hum. Brain Mapp. 29, 751–761.
Silva, A., Cardoso-Cruz, H., Silva, F., Galhardo, V., Antunes, L., 2010. Comparison of anesthetic depth indexes based on thalamocortical local field potentials in rats. Anesthesiology 112, 355–363.
Stamatakis, E.A., Adapa, R.M., Absalom, A.R., Menon, D.K., 2010. Changes in resting neural connectivity during propofol sedation. PLoS One 5, e14224.
Steyn-Ross, D.A., Steyn-Ross, M.L., Wilcocks, L.C., Sleigh, J.W., 2001. Toward a theory of the general-anesthetic-induced phase transition of the cerebral cortex. II. Numerical simulations, spectral entropy, and correlation times. Phys. Rev. E Stat. Nonlin. Soft Matter Phys. 64, 011918.
Steyn-Ross, M.L., Steyn-Ross, D.A., Sleigh, J.W., Whiting, D.R., 2003. Theoretical predictions for spatial covariance of the electroencephalographic signal during the anesthetic-induced phase transition: increased correlation length and emergence of spatial self-organization. Phys. Rev. E Stat. Nonlin. Soft Matter Phys. 68, 021902.
Sumiyoshi, A., Suzuki, H., Ogawa, T., Riera, J.J., Shimokawa, H., Kawashima, R., 2012. Coupling between gamma oscillation and fMRI signal in the rat somatosensory cortex: its dependence on systemic physiological parameters. NeuroImage 60, 738–746.
Tononi, G., 2004. An information integration theory of consciousness. BMC Neurosci. 5, 42.
Tononi, G., 2010. Information integration: its relevance to brain function and consciousness. Arch. Ital. Biol. 148, 299–322.
Tu, Y., Yu, T., Fu, X.Y., Xie, P., Lu, S., Huang, X.Q., Gong, Q.Y., 2011. Altered thalamocortical functional connectivity by propofol anesthesia in rats. Pharmacology 88, 322–326.
Tung, A., Szafran, M.J., Bluhm, B., Mendelson, W.B., 2002. Sleep deprivation potentiates the onset and duration of loss of righting reflex induced by propofol and isoflurane. Anesthesiology 97, 906–911.
Upadhyay, J., Baker, S.J., Chandran, P., Miller, L., Lee, Y., Marek, G.J., Sakoglu, U., Chin, C.L., Luo, F., Fox, G.B., Day, M., 2011. Default-mode-like network activation in awake rodents. PLoS One 6, e27839.
Veselis, R.A., 2001. Anesthesia—a descent or a jump into the depths? Conscious. Cogn. 10, 230–235 (discussion 246–258).
Veselis, R.A., Reinsel, R.A., Feshchenko, V.A., Wronski, M., 1997. The comparative amnestic effects of midazolam, propofol, thiopental, and fentanyl at equisedative concentrations. Anesthesiology 87, 749–764.
Veselis, R.A., Reinsel, R.A., Feshchenko, V.A., 2001. Drug-induced amnesia is a separate phenomenon from sedation: electrophysiologic evidence. Anesthesiology 95, 896–907.
Vincent, J.L., Patel, G.H., Fox, M.D., Snyder, A.Z., Baker, J.T., Van Essen, D.C., Zempel, J.M., Snyder, L.H., Corbetta, M., Raichle, M.E., 2007. Intrinsic functional architecture in the anaesthetized monkey brain. Nature 447, 83–86.
Vincent, J.L., Kahn, I., Snyder, A.Z., Raichle, M.E., Buckner, R.L., 2008. Evidence for a frontoparietal control system revealed by intrinsic functional connectivity. J. Neurophysiol. 100, 3328–3342.
Wang, K., van Meer, M.P., van der Marel, K., van der Toorn, A., Xu, L., Liu, Y., Viergever, M.A., Jiang, T., Dijkhuizen, R.M., 2011. Temporal scaling properties and spatial

synchronization of spontaneous blood oxygenation level-dependent (BOLD) signal fluctuations in rat sensorimotor network at different levels of isoflurane anesthesia. NMR Biomed. 24, 61–67.
Williams, K.A., Magnuson, M., Majeed, W., LaConte, S.M., Peltier, S.J., Hu, X., Keilholz, S.D., 2010. Comparison of alpha-chloralose, medetomidine and isoflurane anesthesia for functional connectivity mapping in the rat. Magn. Reson. Imaging 28, 995–1003.
Zecharia, A., Franks, N.P., 2009. General anesthesia and ascending arousal pathways. Anesthesiology 111, 695–696.
Zhang, N., Rane, P., Huang, W., Liang, Z., Kennedy, D., Frazier, J.A., King, J., 2010. Mapping resting-state brain networks in conscious animals. J. Neurosci. Methods 189, 186–196.
Zhao, F., Zhao, T., Zhou, L., Wu, Q., Hu, X., 2008. BOLD study of stimulation-induced neural activity and resting-state connectivity in medetomidine-sedated rat. NeuroImage 39, 248–260.
Zhou, Y., Shu, N., Liu, Y., Song, M., Hao, Y., Liu, H., Yu, C., Liu, Z., Jiang, T., 2008. Altered resting-state functional connectivity and anatomical connectivity of hippocampus in schizophrenia. Schizophr. Res. 100, 120–132.